SHARP Shock Database

Ganushkina, N.Y.; van de Kamp, M.; Hoppe, T.; Dubyagin, S.; Gedalin, M.; Dimmock, A.; Lalti, A.; Khotyaintsev, Y.V.; Graham, D.B.; Vink, J.; Russell, C.T.

DOI
10.1029/2024JA032625

Publication date
2024

Document Version
Final published version

Published in
Journal of Geophysical Research A: Space Physics

JGR Space Physics

DATA ARTICLE
10.1029/2024JA032625

Special Collection:
Dynamical processes in space plasmas

SHARP Shock Database

N. Y. Ganushkina[1,2], M. van de Kamp[1], T. Hoppe[1], S. Dubyagin[1], M. Gedalin[3], A. Dimmock[4], A. Lalti[4,5], Y. V. Khotyaintsev[4], D. B. Graham[4], J. Vink[6], and C. T. Russell[7]

[1]Finnish Meteorological Institute, Helsinki, Finland, [2]Department of Climate and Space Sciences and Engineering, University of Michigan, Ann Arbor, MI, USA, [3]Department of Physics, Ben Gurion University of the Negev, Beer-Sheva, Israel, [4]Swedish Institute of Space Physics, Uppsala, Sweden, [5]Space and Plasma Physics, Department of Physics and Astronomy, Uppsala University, Uppsala, Sweden, [6]University of Amsterdam, Amsterdam, The Netherlands, [7]Department of Earth, Planetary, and Space Sciences, University of California, Los Angeles, CA, USA

Abstract Despite more than half a century of Collisionless shock (CS) research, our understanding of the processes of the shock energy dissipation into the charge particle heating and acceleration remains incomplete. To help to address the problem of the rate of the data analysis on CSs being well below of the rate of the data acquisition, an open-source high-level database of shocks and a centralized source of advanced tools for the purpose of analyzing shock structure and dynamics have been developed. The database is called SHARP shock database by the name of the project SHARP (Shocks: structure, AcceleRation, dissiPation) funded by the European Union's Horizon 2020 program. The SHARP shock database contains shock crossings and corresponding parameters obtained from Cluster and MMS (Magnetospheric Multiscale) missions for terrestrial bow shocks, THEMIS (Time History of Events and Macroscale Interactions during Substorms)/ARTEMIS (Acceleration, Reconnection, Turbulence and Electrodynamics of the Moon's Interaction with the Sun) missions for interplanetary shocks, and MAVEN (Mars Atmosphere and Volatile EvolutioN) and VEX (Venus Express) missions for shocks at non-magnetized planets. The SHARP shock database can be accessed via https://sharp.fmi.fi/shock-database/.

Plain Language Summary Collisionless Shocks exist at all scales in the Universe: from only one cm in laboratory plasmas to megaparsec scales in galaxy clusters. Shocks are places where the plasma and field go through dramatic changes: in density, temperature, field strength and flow speed. Shocks are collisionsless when collisions are not important. Collisionless shocks are one of the most fundamental phenomena in space and one of the most powerful accelerators in the Universe. The developed database of specific shock parameters obtained from measurements near the Earth, in the interplanetary medium and near Mars and Venus is a tool open to everybody to help to conduct the research on CSs in many environments. The funding for it was received from the European Union's Horizon 2020 program in the project SHARP (Shocks: structure, AcceleRation, dissiPation). The SHARP shock database can be accessed via https://sharp.fmi.fi/shock-database/.

Key Points:

- SHARP shock database is newly-built on measurements from Cluster, MMS, THEMIS/ARTEMIS, MAVEN and VEX missions
- The SHARP database accessible via https://sharp.fmi.fi/shock-database contains shock crossings with shock parameters
- The developed database allows large-scale comparisons of collisionless shocks across a vast array of parameters

Correspondence to:
N. Y. Ganushkina,
ganuna@umich.edu

Citation:
Ganushkina, N. Y., van de Kamp, M., Hoppe, T., Dubyagin, S., Gedalin, M., Dimmock, A., et al. (2024). SHARP Shock Database. *Journal of Geophysical Research: Space Physics*, *129*, e2024JA032625. https://doi.org/10.1029/2024JA032625

Received 9 MAR 2024
Accepted 25 JUN 2024

1. Introduction

Collisionless shocks (CSs) are one of the most fundamental phenomena in space and one of the most powerful accelerators in the Universe. Collisionless Shocks are found in almost every plasma environment observed either directly or indirectly such as: the Earth's bow shock that forms the interface between the solar wind and the terrestrial magnetosphere, bow shocks in the vicinity of other planets, interplanetary shocks that separate different flows within the solar wind, at the boundaries of solar systems or heliospheres, around other stars, supernovae remnants, gamma ray bursts, active galactic nuclei, and clusters of galaxies. CSs exist at all scales in the Universe: from only one cm in laboratory plasmas to megaparsec scales in galaxy clusters.

CSs are, in many aspects, a unique plasma phenomenon. They are the most effective energizers of charged particles capable of accelerating particles to very high energies (even up to $\sim 10^{20}$ eV). CSs are multi-scale objects where the interaction between the electromagnetic fields and charged particles provide the dissipation across all scales, starting with the electron inertial scale within the shock transition layer, and ending with the overall scale of the physical system. Physical processes at all these scales are interrelated. CSs are strongly nonlinear objects where the field-particle interactions are crucial. Understanding physics of CSs is not only necessary for comprehension of the processes taking place in the vicinity of various remote astrophysical objects but also for

advance of our knowledge of most fundamental phenomena in plasmas such as acceleration, dissipation, and transition to irreversibility.

Despite more than half a century of CS research, our understanding of the processes of the shock energy dissipation into the charge particle heating and acceleration remains incomplete. The only region where CSs can be currently probed by in situ measurements is the heliosphere. However, very often the rate of the data analysis is well below of the rate of the data acquisition. Several attempts to develop shock databases have been made using various satellite data. The University of Helsinki's Heliospheric Shock Database (www.ipshocks.fi/) is built for Interplanetary shocks on the measurements from several spacecraft, covering time intervals from the 1970s (Helios A and B) to 2018 (Wind, Advanced Composition Explorer, Cluster and Stereo (Solar TErrestrial RElations Observatory) A and B) and provides the shock crossing times, shock geometry and shock dynamics parameters and Alfvénic Mach number (M_A). A database on terrestrial bow shock crossings can be found at the Cluster Science Archive (https://www.cosmos.esa.int/web/csa/bow-shock-magnetopause-crossings) which contains 529 events observed by Cluster spacecraft between years 2001 and 2013 (Kruparova et al., 2019). Meanwhile, a centralized shock database with the relevant advanced tools for the efficient exploitation of data is missing.

The main scientific objective of the project called SHARP (SHocks: structure, AcceleRation, dissiPation) (https://sharp.fmi.fi/) which received funding from the European Union's Horizon 2020 research and innovation program was to achieve a major leap in the understanding of the structure of CSs in various environments and of the acceleration processes at all shock scales. One of the major goals was to develop an open-source high-level database of shocks and a centralized source of advanced tools for the purpose of analyzing shock structure and dynamics. The current paper presents the newly-developed SHARP shock database built with general structure described in Section 2 using the measurements from Cluster, MMS (Magnetospheric Multiscale), THEMIS (Time History of Events and Macroscale Interactions during Substorms)/ARTEMIS (Acceleration, Reconnection, Turbulence and Electrodynamics of the Moon's Interaction with the Sun), MAVEN (Mars Atmosphere and Volatile EvolutioN) and VEX (Venus Express) missions (details given in Section 3). Section 3 lists all the shock parameters included in the SHARP shock database and provides the description of the methods of the determination of these parameters. Section 4 briefly describes the usage of the SHARP shock database which has been done so far, and summarizes the contribution of the database into facilitation of more efficient shock studies and enhancement of the collaboration.

2. SHARP Shock Database: General Structure and Access

The SHARP shock database can be accessed via https://sharp.fmi.fi/shock-database/. There are several ways to build the outputs from it (see Figure 1). First option for a user is to download the entire database of shocks in as XML or CSV files or/and to download the plots of all shocks available in the database as TAR archive file. This option does not require selection of specific satellite data or any shock parameters.

The second option is to build a user-defined shock database. To see a list of all available data (6,112 shocks), a user can simply click on “Submit” button. To create any specific output from the SHARP shock database, a user can select spacecraft mission/missions and/or adjust any parameter range, before clicking “Submit.” The following missions can be selected: MMS for terrestrial bow shocks, MAVEN for Martian bow shocks, VEX for Venusian bow shocks, THEMIS B and C (ARTEMIS since 2010) for interplanetary shocks, and Cluster for terrestrial bow shocks. Note that if none of the specific satellites is selected, the data from all of them will be included.

Burst data mode is available only for MMS data, so “Data mode” button is set to “All data.” “Inbound” from upstream to downstream and/or “Outbound” directions for shock crossing can be selected but **if** no direction is chosen, all will be included (the option “Include shocks without direction value” is pre-checked, see Figure 1).

Figure 2 presents the list of the shock parameters included in the SHARP shock database with pre-defined ranges. The details on the shock parameters and their calculations are given in Section 3. If “Include shocks without (specific parameter) value” for a certain parameter is unchecked, shocks where the corresponding parameter value is unavailable will not be included. It is not recommended to use the “back” and “forward” buttons on the browser, as the website may not work properly while using them.

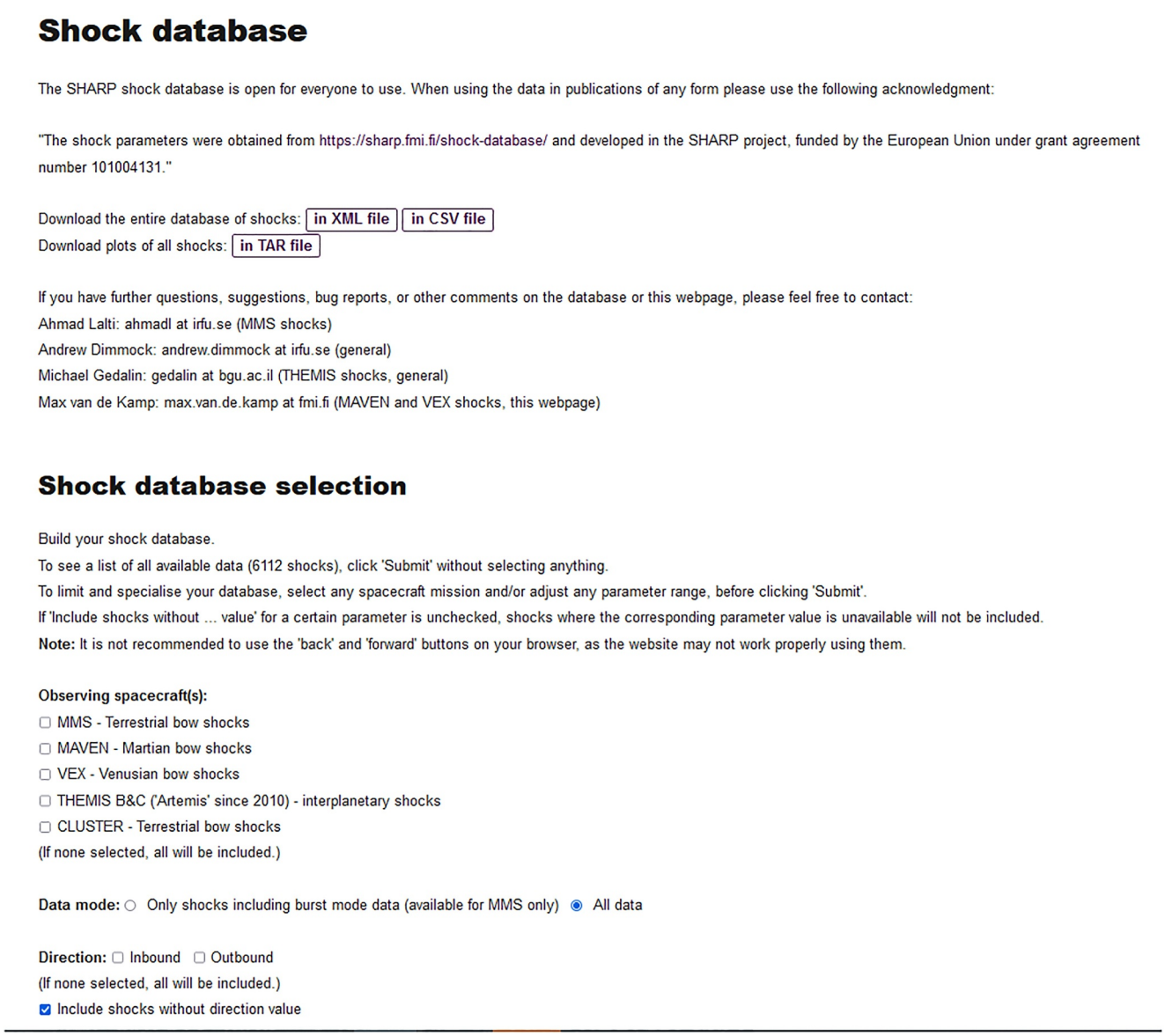

Shock database

The SHARP shock database is open for everyone to use. When using the data in publications of any form please use the following acknowledgment:

"The shock parameters were obtained from https://sharp.fmi.fi/shock-database/ and developed in the SHARP project, funded by the European Union under grant agreement number 101004131."

Download the entire database of shocks: in XML file | in CSV file
Download plots of all shocks: in TAR file

If you have further questions, suggestions, bug reports, or other comments on the database or this webpage, please feel free to contact:
Ahmad Lalti: ahmadl at irfu.se (MMS shocks)
Andrew Dimmock: andrew.dimmock at irfu.se (general)
Michael Gedalin: gedalin at bgu.ac.il (THEMIS shocks, general)
Max van de Kamp: max.van.de.kamp at fmi.fi (MAVEN and VEX shocks, this webpage)

Shock database selection

Build your shock database.
To see a list of all available data (6112 shocks), click 'Submit' without selecting anything.
To limit and specialise your database, select any spacecraft mission and/or adjust any parameter range, before clicking 'Submit'.
If 'Include shocks without ... value' for a certain parameter is unchecked, shocks where the corresponding parameter value is unavailable will not be included.
Note: It is not recommended to use the 'back' and 'forward' buttons on your browser, as the website may not work properly using them.

Observing spacecraft(s):
- ☐ MMS - Terrestrial bow shocks
- ☐ MAVEN - Martian bow shocks
- ☐ VEX - Venusian bow shocks
- ☐ THEMIS B&C ('Artemis' since 2010) - interplanetary shocks
- ☐ CLUSTER - Terrestrial bow shocks

(If none selected, all will be included.)

Data mode: ○ Only shocks including burst mode data (available for MMS only) ◉ All data

Direction: ☐ Inbound ☐ Outbound
(If none selected, all will be included.)
☑ Include shocks without direction value

Figure 1. Options for building of outputs from the SHARP shock database at https://sharp.fmi.fi/shock-database/.

Figure 3 shows the output from the SHARP shock database when no specific spacecraft is selected and no parameter is adjusted. The output include all available data MMS, MAVEN, VEX, THEMIS, and CLUSTER satellites in both inbound and outbound directions. The selection can be modified at this step by clicking on the "Return to the selection form" button. The shock parameters for this selection can be downloaded in the XML and CSV file formats, whereas the shock plots can be downloaded in the TAR archive file format. The downloadable XML and CSV files contain the user data about the database, such as the sources of all the raw data and the methods used to develop the database. To start again from scratch, a user needs to click on "Clear all selections' button.

The output from the SHARP shock database is shown as a table (seen in the bottom of Figure 3) which contains date and time, spacecraft name, and all the available shock parameters with burst mode interval (MMS only) and direction (In and Out). The full name of the parameter appears when the cursor arrow is moved to the parameter's symbol in the table. The last column in the table is the plot of corresponding data used to determine the shock parameters for that particular shock. Clicking on it will allow to see the full plot.

Adjust one or more parameter ranges:

(The pre-filled default values correspond to the lowest and highest values in the current database.)

		Lower limit	Upper limit	
	Date / time	15/01/2001 00.00	12/12/2020 23.59	Include shocks without date/time value
ΔR	Separation between observations of same constellation ○ min ○ mean ◉ max	3.4 km	17162 km	Include shocks without ΔR value
M_A	Shock Alfvén Mach number	0	150	Include shocks without M_A value
M_f	Shock fast mode Mach number	1	53	Include shocks without M_f value
θ_{Bn}	Angle between the shock normal and upstream magnetic field	0 deg	90 deg	Include shocks without θ_{Bn} value
$\|V_{us}\|$	Plasma velocity magnitude upstream of the shock	20 km/s	14410 km/s	Include shocks without $\|V_{us}\|$ value
$\|B_{us}\|$	Magnetic field magnitude upstream of the shock	0 nT	63 nT	Include shocks without $\|B_{us}\|$ value
N_{us}	Plasma density upstream of the shock	0 cm^{-3}	163 cm^{-3}	Include shocks without N_{us} value
$T_{i,us}$	Ion temperature upstream of the shock	0.7 eV	95.8 eV	Include shocks without $T_{i,us}$ value
β_{us}	Ion plasma beta upstream of the shock	0	88.9	Include shocks without β_{us} value
P_{us}	Dynamic pressure upstream of the shock	0 nPa	24 nPa	Include shocks without P_{us} value
R_{cB}	Magnetic compression ratio $\|B_{ds}\|/\|B_{us}\|$	0	61	Include shocks without R_{cB} value
R_{cn}	Plasma density compression ratio N_{ds}/N_{us}	0	5640	Include shocks without R_{cn} value
R_{cT}	Electron temperature compression ratio $T_{e,ds}/T_{e,us}$	1	10	Include shocks without R_{cT} value

Submit

Figure 2. Shock parameters which ranges can be chosen (pre-defined values for ranges shown) included in the SHARP shock database.

3. Spacecraft Data Used for Database Development and Calculations of Shock Parameters

The SHARP shock database contains information about terrestrial shocks, interplanetary shocks and shocks at non-magnetized planets (Venus and Mars). The shock parameters which can be obtained depend on the available measurements in corresponding regions. The database contains the parameters which ranges can be chosen and the parameters which are pre-determined. Below is the list of shock parameters with adjustable ranges (Figure 2):

- Date [day.month.year]/Time UT [hours. minutes]: interval for shock measurements to output;
- ΔR [km]: Separation distance between observations of same constellation of satellites. Either the minimum, maximum or mean of all separations can be selected.
- M_A: Shock Alfvén Mach number;
- M_f: Shock fast mode Mach number;
- θ_{Bn} [deg]: Angle between the shock normal **n** and upstream magnetic field $\mathbf{B}_{us}$;
- $|V_{us}|$ [km/s]: Plasma velocity magnitude upstream of the shock;
- $|B_{us}|$ [nT]: Magnetic field magnitude upstream of the shock;
- N_{us} [cm^{-3}]: Plasma density upstream of the shock;
- $T_{i,us}$ [eV]: Ion temperature upstream of the shock;
- β_{us}: Ion plasma beta upstream of the shock;
- P_{us} [nPa]: Dynamic pressure upstream of the shock;

Shock database selection

You have selected:

Observing spacecraft mission(s): MMS, MAVEN, VEX, THEMIS, CLUSTER
Data mode: All data
Direction: Inbound, Outbound

Modify your selection: Return to the selection form

Download the parameters of these shocks: in XML file | in CSV file
Download plots of these shocks (this may take a moment): in TAR file

Or, to start again from scratch: Clear all selections

Note: It is not recommended to use the 'back' and 'forward' buttons on your browser, as the website may not work properly using them.

For more information about the database, such as the sources of all the raw data and the methods used to develop this database, please see the user data in the downloadable XML- or CSV-files.
If you have further questions, suggestions, bug reports, or other comments on the database or this webpage, please feel free to contact:
Webpage: Max van de Kamp: max.van.de.kamp at fmi.fi; Theresa Hoppe: theresa.hoppe at fmi.fi
SHARP project: Natalia Ganushkina: nataly.ganushkina at fmi.fi
MMS shocks: Ahmad Lalti: ahmadl at irfu.se
THEMIS and CLUSTER shocks: Michael Gedalin: gedalin at bgu.ac.il
MAVEN and VEX shocks: Max van de Kamp: max.van.de.kamp at fmi.fi

Selected shocks (6112 of 6112):

date & time	Spacecraft	max ΔR (km)	Burst mode interval	Direction	M_A	M_f	θ_{Bn} (deg)	$\lvert V_{us}\rvert$ (km/s)	$\lvert B_{us}\rvert$ (nT)	N_{us} (cm^{-3})	$T_{i,us}$ (eV)	β_{us}	P_{us} (nPa)	R_{cB}	R_{cn}	R_{cT}	Plot preview Click to see plot.
2015-10-07 11:19:10	MMS	30.5	11:18:14 - 11:20:13	Out	6.79	4.58	71.61	421.3	14.381	27.67	11.51	0.620	9.81	3.37	4.51	2.47	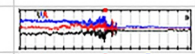
2015-10-07 11:35:08	MMS	30.6	11:34:24 - 11:38:03	In	8.95	5.51	87.60	423.3	12.641	36.89	7.76	0.721	13.24	3.70	4.14	3.18	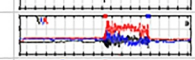
2015-10-07 11:37:24	MMS	30.6	11:34:24 - 11:38:03	Out	8.95	5.45	89.89	424.7	12.828	37.71	8.23	0.759	13.62	3.70	4.20	3.20	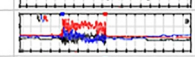
2015-10-07 11:44:39	MMS	30.6	11:44:14 - 11:45:23	In	7.90	4.93	86.15	425.7	13.749	33.82	10.56	0.761	12.27	3.41	4.67	3.37	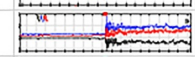
2015-10-07 12:07:10	MMS	30.6	12:06:04 - 12:09:43	Out	5.07	4.17	70.60	424.5	17.859	23.68	7.38	0.221	8.54	3.19	5.40	2.79	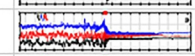
2015-10-07 12:54:16	MMS	30.5	12:53:54 - 12:55:13	In	6.93	4.90	74.12	419.0	15.270	33.79	7.84	0.457	11.89	3.38	6.10	3.11	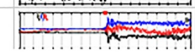

Figure 3. SHARP shock database output when no specific spacecraft is selected and no parameter is adjusted.

- R_{cB}: Magnetic compression ratio $|B_{ds}|/|B_{us}|$;
- R_{cn}: Plasma density compression ratio N_{ds}/N_{us};
- R_{cT}: Electron temperature compression ratio $T_{e,ds}/T_{e,us}$

The SHARP shock database output files also contain other parameters which depend on the satellite data used. Not all parameters can always be computed, for example, if the spacecraft separation is inappropriate (e.g., shock speed). In these cases, the parameter(s) will be flagged. Some parameters are never available for some of the missions.

The SHARP shock database output file contains the following parameters, in addition to the parameters which ranges can be chosen:

- direction (a flag indicating if the shock is inbound (1) or outbound (−1));
- $burst_{start}$ and $burst_{end}$ for the burst mode interval in epoch time (MMS data only);

Table 1
Availability of the SHARP Shock Database Parameters

Parameter/Mission	CLUSTER	MMS	THEMIS	MAVEN	VEX
Time	√	√	√	√	√
Direction	√	√	√	√	√
Burst interval		√			
$\mathbf{B}_{us}$	√	√	√	√	√
$\sigma(\|B_{us}\|)$		√			
$\Delta\theta_B$		√			
N_{us}	√	√	√	√	
$T_{i,us}$		√			
$\mathbf{V}_{us}$	√	√	√	√	
β_{us}		√			
P_{us}		√			
θ_{Bn}	√	√	√	√	√
$\sigma(\theta_{Bn})$		√			
n	√	√	√	√	√
M_A	√	√	√	√	
$\sigma(M_A)$		√			
M_f		√			
$\sigma(M_f)$		√			
R_{cB}	√	√	√	√	√
R_{cn}		√	√		
R_{cT}		√			
Position	√	√		√	√
ΔR	√	√			
TQF		√			
Quick-look plots	√	√	√	√	√

- components B_{xus}, $B_{y_{us}}$ and $B_{z_{us}}$ [nT] of magnetic field upstream of the shock;
- standard deviation on the magnitude of the upstream magnetic field;
- $\Delta\theta_B$, the maximum rotation of the upstream magnetic field vector in the OMNI interval used;
- components V_{xus}, $V_{y_{us}}$ and $V_{z_{us}}$ [km/s] of the plasma velocity upstream of the shock;
- standard deviation of θ_{Bn} based on variation in upstream B in the OMNI interval used;
- components n_x, n_y, and n_z of the shock normal;
- standard deviation of M_A based on variation in upstream B in the OMNI interval used;
- standard deviation of M_f based on variation in upstream B in the OMNI interval used;
- X_{GSE}, Y_{GSE}, and Z_{GSE} coordinates [km] of the spacecraft, when it observed the shock;
- TQF, Tetrahedron quality factor.

The upstream and downstream intervals are marked on the plots of shocks in the relevant database sections (MAVEN, VEX, THEMIS, and Cluster). The lengths of intervals cannot be defined a priori since shocks are very different. The upstream region may be long and quiet but may be short and noisy. Relaxation to a quiet downstream state, if any, may be very slow. For MMS shocks, OMNI data is used for the upstream parameters, and a complex elaborated procedure is applied for finding medians of the distributed values.

Table 1 shows the list of all parameters with marking of which parameters can be available for which missions. The details of parameters for different satellite data are given in the following sections.

3.1. Terrestrial Shocks

To build a comprehensive catalog of terrestrial bow shock crossings with their relevant fundamental parameters, the data from Cluster and MMS were used.

3.1.1. Cluster Shocks

The Cluster mission was launched in 2000 and it consists of four identical spacecraft on similar elliptical polar orbits with an initial perigee at about 4 R_E (R_E = 6,371 km is the Earth's radius) and an apogee at 19.6 R_E (Escoubet et al., 2001). We employed the list of shock crossing observed by Cluster CS1 complied by Kruparova et al. (2019) for the years of 2001–2013. To obtain the upstream and downstream shock parameters for each crossing, we used the magnetic field data from FGM (Fluxgate Magnetometer) experiment (Balogh et al., 2001) in full resolution, the data from Cluster Ion Spectrometry (CIS) Hot Ion Analyzer sensor (Rème et al., 2001) for the ion number densities and flow velocities and the data from the Waves of High frequency and Sounder for Probing of Electron density by Relaxation (WHISPER) sounder (Trotignon et al., 2001) for the electron number densities. The temperature data from Cluster/CIS was not used since the CIS particle data for the solar wind is not reliable, as was noted by Gedalin et al. (2021). Several methods were used for the determination of the shock normal $\hat{\boldsymbol{n}}$. The model normal by Farris and Russell (1994) requires only the position of the spacecraft at the shock crossing. The coplanarity methods (Schwartz, 1998) are based on the coplanarity theorem stating that the measured upstream, $\boldsymbol{B}_u$, and downstream, $\boldsymbol{B}_d$, magnetic field vectors, the difference of the measured downstream $\boldsymbol{V}_2$ and upstream $\boldsymbol{V}_1$ plasma velocity vectors, and the shock normal are all in one plane. These method require identification of the upstream and downstream regions, used for averaging of the required vectors. This identification was done visually for each shock, and the shock normal was determined using mixed coplanarity as follows

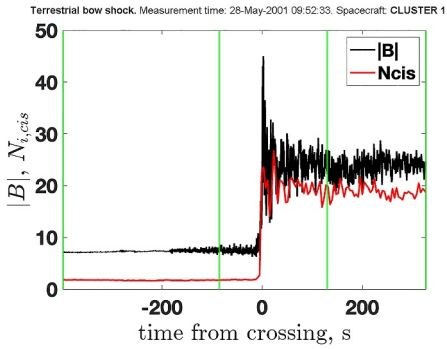

Figure 4. Example of a plot of the terrestrial bow shock, measured by CLUSTER CS1. Shown are the magnetic field magnitude and the Cluster Ion Spectrometry measured ion density. The vertical green lines denote the chosen upstream and downstream regions used in the analysis.

$$\hat{\boldsymbol{n}} = \frac{(\Delta \boldsymbol{B} \times \Delta \boldsymbol{V}) \times \Delta \boldsymbol{B}}{|(\Delta \boldsymbol{B} \times \Delta \boldsymbol{V}) \times \Delta \boldsymbol{B}|} \quad (1)$$

where $\Delta \boldsymbol{B} = \boldsymbol{B}_d - \boldsymbol{B}_u$ and $\Delta \boldsymbol{V} = \boldsymbol{V}_2 - \boldsymbol{V}_1$. The mixed coplanarity normal correlated well with the model normal, so the model normal was chosen as a global shock normal, insensitive to the fine structure of the shock front. The model shock normal was used for determination of the shock angle

$$\theta_{Bn} = \cos^{-1}\frac{|\hat{\boldsymbol{n}} \cdot \boldsymbol{B}_u|}{|\boldsymbol{B}_u|} \quad (2)$$

Determination of the Mach number requires knowledge of the upstream n_u and downstream n_d densities:

$$V_A = \frac{B_u}{\sqrt{4\pi n_u m_p}}, \quad (3)$$

$$V_{sh} = \frac{(n_d \boldsymbol{V}_2 - n_u \boldsymbol{V}_1) \cdot \hat{\boldsymbol{n}}}{n_d - n_u} \quad (4)$$

$$V_u = \frac{n_d}{n_d - n_u}|(\boldsymbol{V}_1 - \boldsymbol{V}_2) \cdot \hat{\boldsymbol{n}}| \quad (5)$$

Here V_A is the upstream Alfvén speed, V_{sh} is the shock speed in the spacecraft frame, and V_u is the upstream plasma speed in the Normal Incidence Frame, in which the upstream plasma velocity is along the shock normal. The densities derived from WHISPER measurements were used in the cases where CIS data were unreliable.

Figure 4 gives an example of a plot of the terrestrial bow shock as measured by CLUSTER CS1, and available in the SHARP database. In this case the CIS density measurements are good and were used for the Mach number determination.

3.1.2. MMS Shocks

The four-spacecraft MMS mission (Burch et al., 2016) was launched on 12 March 2015 in a 28° equatorial inclination, 12 R_E apogee elliptical orbit. Lalti et al. (2022) have compiled the set of 2,797 shock crossings with main shock parameters observed by MMS. The crossings were determined by applying the supervised machine learning technique (Olshevsky et al., 2021). Measurements of the ion velocity distribution functions from Dual Ion Spectrometers of the Fast Plasma Investigation (FPI) suite (Pollock et al., 2016) were used to develop a 3D Convolutional Neural Network (CNN). The developed CNN is able to identify the regions which MMS is crossing based only on the ion energy distributions. The shock parameters for the identified shock crossings included ones related to the spacecraft and data acquisition mode, and the others related to actually shock crossings. The vector normal to the shock $\hat{\boldsymbol{n}}$ is calculated using the bow shock model by Farris and Russell (1994). For the main shock parameters (Alfvénic Mach number M_A, fast mode Mach number M_f, the angle between the upstream magnetic field and the shock normal θ_{Bn}, and the upstream plasma beta β_{us}), the time-shifted OMNI database data from spacecraft located upstream of MMS (https://omniweb.gsfc.nasa.gov/). In addition, the following parameters are also included: the upstream velocity, density, ion temperature, magnetic field vector, magnetic field magnitude, and the solar wind dynamic pressure for each shock crossing. For compression ratios, the downstream shock parameters are calculated using MMS FPI data. Figure 5 gives an example of a plot of the terrestrial bow shock as measured by MMS 1, and available in the SHARP database.

It is possible to calculate the bow shock parameters using in situ MMS data. However, there are some challenges to implement this reliably from a statistical standpoint. MMS instruments were designed to function optimally inside the magnetosphere, which can lead to inaccuracies incurred on solar wind ion moments. The reason is that the narrow and cold solar wind beam is only captured in a limited number of energy bins. For this reason, the MMS shock database uses OMNI data that originates from spacecraft that were intended to measured the solar wind, for the upstream plasma parameters.

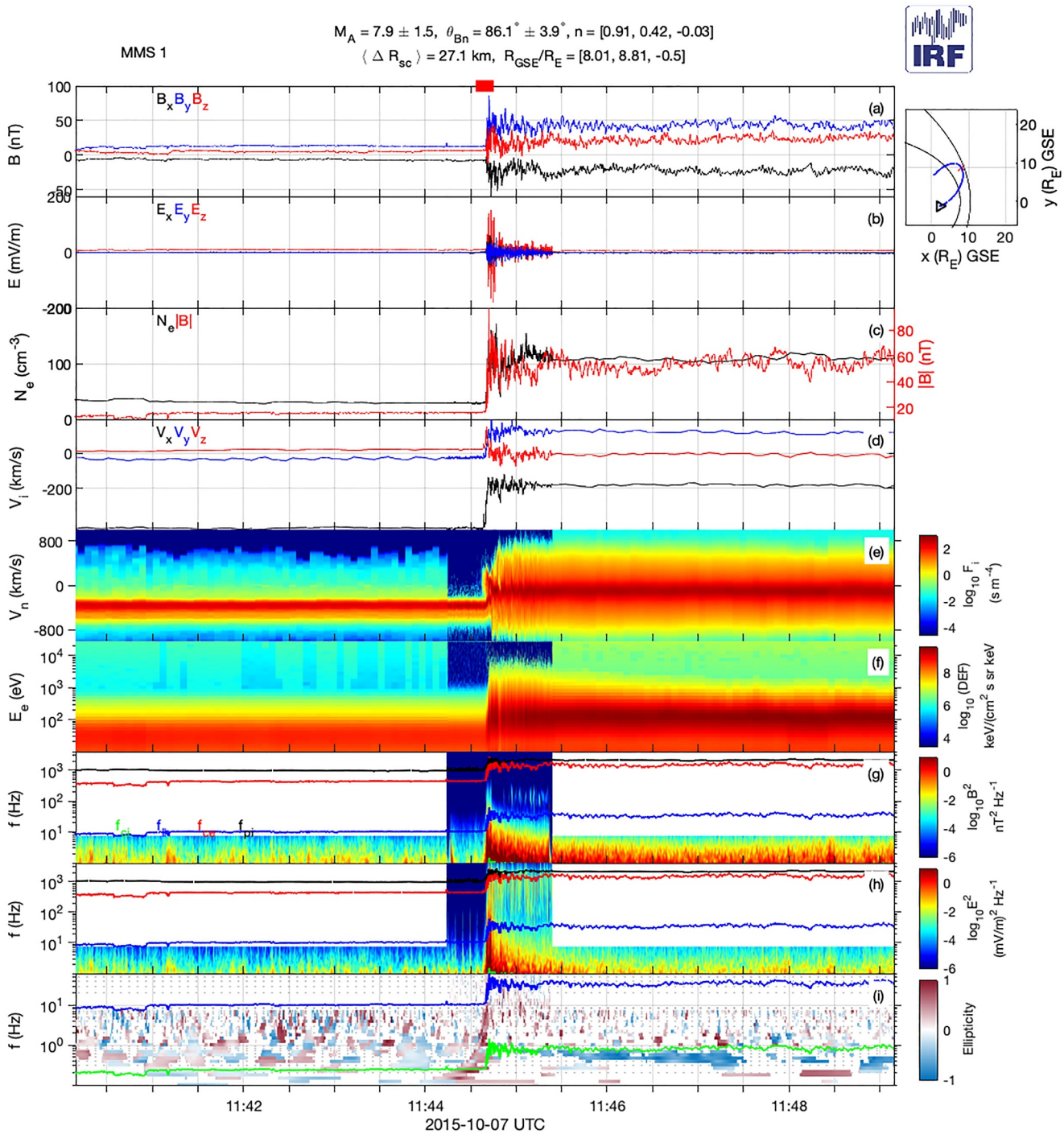

Figure 5. Example of a plot from https://sharp.fmi.fi/shock-database/ of the terrestrial bow shock, measured by MMS 1. Top to bottom: Magnetic field, electric field, electron density, ion velocity, ion velocity distribution function in the normal direction, electron flux energy spectrum, magnetic field power frequency spectrum, electric field power frequency spectrum, and ellipticity.

The mean magnetic field magnitude upstream of the shock is obtained directly from the data for terrestrial shocks using FGM measurements in the full resolution mode onboard MMS and Cluster. For the terrestrial shocks, all vector quantities are in the Geocentric Solar ecliptic coordinate system. The SHARP database contains 2,797 terrestrial shocks measured by MMS between October 2015 and December 2020, and 2,472 measured by

CLUSTER between January 2001 and December 2012. The shock parameters available in the SHARP shock database for CLUSTER and MMS data are shown in Table 1.

3.2. Interplanetary Shocks

The THEMIS mission (Angelopoulos, 2008) was launched on 17 February 2007, and employed five identical spacecraft on elliptical, nearly equatorial orbits lined up at apogee every 4 days. THEMIS was designed to study substorms in the Earth's magnetosphere. In 2009–2011, two of THEMIS's probes, B and C, were sent into lunar orbit as part of a new mission under the name ARTEMIS (Acceleration, Reconnection, Turbulence and Electrodynamics of the Moon's Interaction with the Sun) (Angelopoulos, 2011). ARTEMIS's mission is to study the Earth-Moon Lagrange points, the solar wind, the Moon's plasma wake, and the interaction between Earth's magnetotail and the Moon's own weak magnetism. The two spacecraft, orbiting in opposite directions around the Moon, provide the first 3D measurements of the Moon's magnetic field allowing to determine its regional influence on solar wind particles. Spending more than 70% of orbit time in the solar wind, these satellites provide also a good source of measurements of interplanetary shocks.

The data measured by the spacecraft which are used for the shock analysis include the magnetic field vector, and the velocity vector and density of both ions and electrons. The Fluxgate Magnetometer (FGM) (Auster et al., 2008) measures the ambient magnetic field and its low frequency fluctuations, up to 64 vectors/sec. The Elecrostatic Analyzer (ESA) (McFadden et al., 2008) measures the electron and ion distributions in 32 energy channels and 88 angle channels. A full distribution is provided at best at 32 spin cadence, while a reduced distribution is provided at 1 spin cadence. The distributions moments are calculated onboard.

From these, the upstream and downstream values of these parameters were calculated. Identification of suitable upstream and downstream regions was done visually for each shock, as was done for Cluster shocks. The Alfvenic Mach number M_A, the shock normal $\hat{\boldsymbol{n}}$ and the shock angle θ_{Bn} are calculated using mixed coplanarity, as for Cluster shocks above, when the density and velocity are taken from electron measurements. In the upstream and downstream regions the electron and ion densities are expected to be equal, as well as the electron and ion velocity vectors. In the solar wind, the ion distribution is a cold beam, and the measurements of the ion parameters are often unreliable. The electron parameters were found more reliable for interplanetary shocks measured by Artemis. The upstream magnetic field and electron density and velocity are stored in the database. All vectors are expressed in the Despun Sun-pointing L-momentum (DSL) coordinate system. Figure 6 gives an example of a plot of an interplanetary shock as measured by THEMIS B, and available in the SHARP database. The SHARP database contains 407 interplanetary shocks measured by THEMIS B and C/ARTEMIS, between June 2008 and November 2019. Table 1 shows the shock parameters available in the SHARP shock database for THEMIS/ARTEMIS data.

3.3. Shocks at Non-Magnetized Planets

Mars and Venus, unlike other planets, do not have global intrinsic magnetic fields. As such, they form a non-magnetized obstacle in the solar wind, and the solar wind magnetic field drapes about the planet, piling up on the dayside, creating an induced magnetosphere.

The bow shocks are formed much closer to the planets, therefore, their geometrical scale is much smaller than in the terrestrial bow shock, and, although not caused by an intrinsic magnetosphere, magnetic effects are involved. These bow shocks as measured by MAVEN (for Mars) and VEX (for Venus) are analyzed in the SHARP project. The calculations involved to analyze these shocks in this project have not yet been published elsewhere, and are therefore described in this paper in more detail than those of the other missions.

MAVEN mission, launched in 2013, is observing the Martian upper atmosphere (Gruesbeck et al., 2018). Its goal is to determine the role that loss of atmospheric gas to space played in changing the Martian climate through time. The Solar Wind Ion Analyzer (Halekas et al., 2015) measures the ion distributions at 4 s cadence, in the energy range 5 eV–25 keV, and with a field of view of $360° \times 90°$. The distributions moments, that is, the velocity vector and ion density of the plasma, assuming all ions are protons, are calculated onboard. The magnetometer MAG (Connerney et al., 2015) measures the ambient magnetic field vector at the intrinsic rate of 32 samples/second. The data, in addition to the spacecraft location, are downloaded from the AMDA Versatile web tool for Space Physics (http://amda.cdpp.eu). All parameters are given in the Mars Solar Orbital (MSO) coordinate system. In

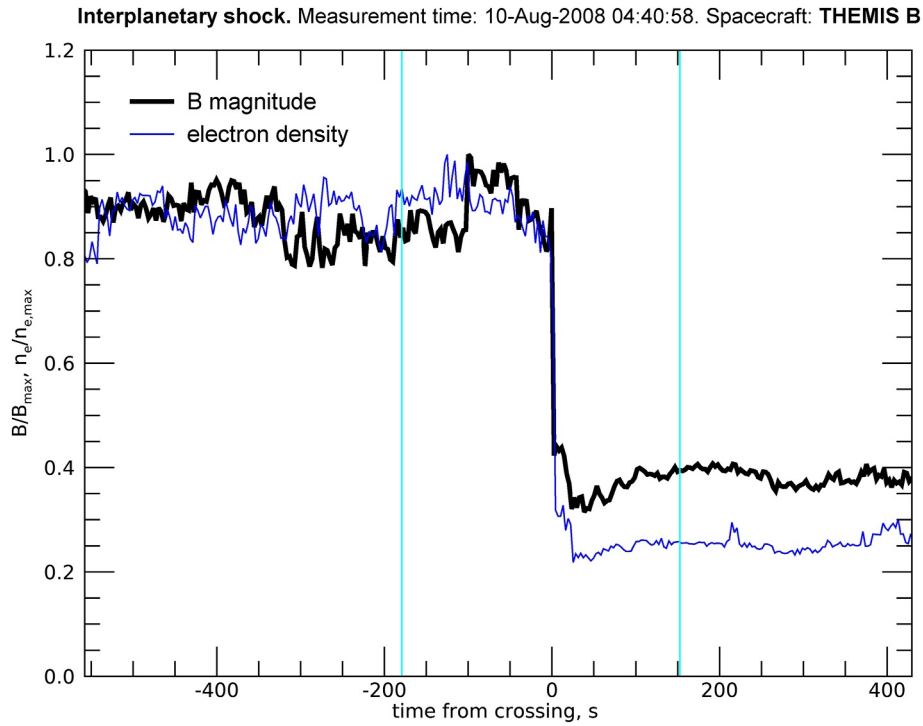

Figure 6. Example of a plot of an interplanetary shock, measured by THEMIS B. Shown are magnetic field magnitude and the electron density, both relative to their maximum value around the shock. The vertical green lines mark the upstream and downstream regions used for the shock parameter determination.

this system, the x-axis points from Mars to the Sun. The y-axis lies in the plane of the Mars-Sun vector and the orbital velocity vector, orthogonal to the x-axis, and quasi-antiparallel to the orbital velocity. The z-axis completes the right-hand system.

The list of MAVEN shock measurement times was obtained from Garnier (2022). For each of these shocks times, the measured data were analyzed over a period of 20 min centered around the shock time. The upstream measurement interval was selected as the 2-min period within the 10-min upstream side, where the time average of magnetic field magnitude multiplied by ion density is smallest. From this interval, the upstream magnetic field $\mathbf{B}_{us}$, ion velocity $\mathbf{V}_{us}$ and density N_{us} are calculated as the averages of the respective time-dependent parameters over this interval. The downstream measurement interval is difficult to select based on any particular parameter-value condition; therefore, this is selected as the period between 6 and 8 min downstream of the shock. The downstream plasma parameters $\mathbf{B}_{ds}$, $\mathbf{V}_{ds}$ and N_{ds} are calculated as averages over this interval.

In order to find the shock normal, a model for the Martian bow shock is used. For this, it is useful to first convert the location data of MAVEN to the aberrated MSO system. With respect to the MSO system, this system is slightly rotated about the z-axis, to account for the relative motion of Mars to the average solar wind direction:

$$\begin{aligned} x_a &= x\cos\psi - y\sin\psi \\ y_a &= x\sin\psi + y\cos\psi \\ z_a &= z \end{aligned} \tag{6}$$

with x, y and z the location of the measurement point of the shock in MSO coordinates, and x_a, y_a and z_a in the aberrated MSO coordinates, and $\psi = 4°$ the aberration (rotation) angle.

The bow shock is modeled as a surface of revolution of a conic section. Hall et al. (2016, 2019) found that when fitting this model to measurements, the focus location and eccentricity of the shape stayed roughly constant while the semilatus rectum varies. The two former parameters are therefore taken constant, with as values the averages of the values found by Hall et al. (2016, 2019), which gives the focus location on the x_a-axis $x_0 = 0.75R_M$ (with R_M

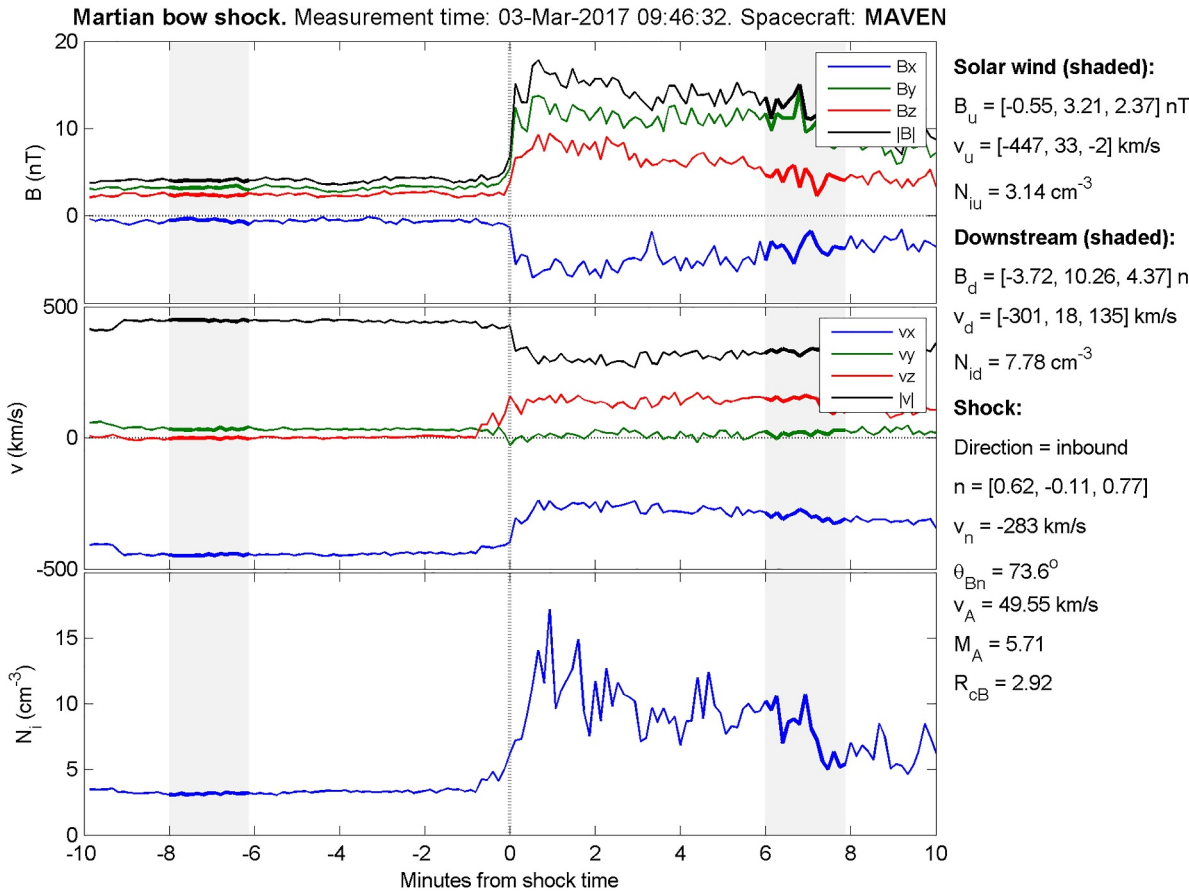

Figure 7. Example of a plot of the Martian bow shock, measured by MAVEN. Upper panel: magnetic field strength. Middle panel: ion velocity. Lower panel: ion density.

the radius of Mars) and the eccentricity $\varepsilon = 1.01$ (the latter making the shape very close to a paraboloid). With these, the semilatus rectum L can be calculated from the location of any point at the shock surface, defining the entire shock surface at that point in time. This surface can be characterized by the terminator distance R_{TD} of the bow shock (Hall et al., 2016), which is given by:

$$R_{TD} = \sqrt{(x_a - x_0)^2 + y_a^2 + z_a^2 + \varepsilon^2 x_a^2 - x_0^2 + 2\varepsilon x_a \sqrt{(x_a - x_0)^2 + y_a^2 + z_a^2}} \tag{7}$$

The shock normal (in the aberrated coordinates) $\mathbf{n}_a$ can then be calculated as:

$$\mathbf{n}_a = [-\sin\alpha,\ \cos\alpha\cos\phi,\ \cos\alpha\sin\phi] \tag{8}$$

with:

$$\alpha = \arctan\frac{-\varepsilon\left(\sqrt{x_0^2 + R_{TD}^2} - \varepsilon x_a\right) - x_a + x_0}{\sqrt{\left(\sqrt{x_0^2 + R_{TD}^2} - \varepsilon x_a\right)^2 - (x_a - x_0)^2}} \tag{9}$$

$$\phi = \arctan\frac{z_a}{y_a} \tag{10}$$

The shock normal in non-aberrated MSO coordinates **n** is found by applying the inversion of Equation 6 to $\mathbf{n}_a$. Figure 7 gives an example of a plot of the Martian bow shock as measured by MAVEN, and available in the SHARP database.

VEX (Zhang et al., 2006) was ESA's first spacecraft to voyage to Venus; it was built around the design of Mars Express. It studied the planet's complex dynamics and chemistry, and the interactions between the atmosphere and the surface, which provided clues about the surface's characteristics. VEX orbited Venus from 2006 to 2014, providing a sufficiently long duration of observations to give an opportunity to investigate the effects of solar activity on the Venusian bow shock. VEX had a highly elliptical polar orbit with a periapsis of 250–300 km altitude at 78°N, and crossed the bow shock twice a day. In addition, VEX covered a large range of Solar Zenith Angles (from ∼10° to ∼135°) at the Venusian bow shock, which is suitable to determine the bow shock locations at both the stand-off and terminator distances.

The magnetometer MAG onboard of VEX consisted of two fluxgate sensors for a separation of magnetic effects of the spacecraft origin from the ambient space magnetic field. The Ion Mass Analyzer (IMA), part of the Analyzer of Space Plasmas and EneRgetic Atoms (ASPERA-4), measured ion densities and velocities. Both MAG and IMA data were obtained from the AMDA Versatile web tool for Space Physics. The B-field data have a time resolution of 4 s. Unfortunately, the ion density and velocity data are available at a low time resolution only (192 s).

The observations are presented in the Venus Solar Orbital (VSO) coordinates. In this system, the x-axis points from Venus to the Sun. The y-axis lies in the plane of the Venus-Sun vector and the orbital velocity vector, orthogonal to the x-axis, and quasi-parallel to the orbital velocity. The z-axis completes the right-hand system. Note that this means that the y- and z-axes are oriented opposite to their equivalent in the MSO system.

The SHARP shock database includes two lists of the shocks measured by VEX (Shan et al., 2015), one measured during a solar minimum period and the other during a solar maximum period. For each of these shocks times, the shock normal is determined in a similar way as for the MAVEN data. The location data of VEX are converted to an aberrated VSO coordinate system to correct for the solar wind direction relative to the planet's motion (see Equation 6), with $\psi = -4.7°$. The bow shock model is similar to the Martian one, that is, a surface of revolution of a conic section, where the focus location and eccentricity stay relatively constant while the semilatus rectum varies with time. Shan et al. (2015) found from the VEX data $x_0 = 0.596R_V$ (R_V being the radius of Venus) and $\varepsilon = 1.03$ during solar minimum, and $x_0 = 0.775R_V$ and $\varepsilon = 1.096$ during solar maximum; these values are also used for the respective subsets of the shock list here. The shock normal **n** at each measurement is determined following the same steps as in the case of Mars; see above.

For each shock, the measured data are analyzed over a period of 20 min centered around the shock time. The length of averaging periods for the up-and downstream B-field values is this time chosen as 192 s, to match the time resolution of the **V** and N measurements. The upstream measurement interval is selected as the 192 s period within the 10-min upstream side, where the time average of magnetic field magnitude |**B**| is smallest. From this interval, the upstream magnetic field vector $\mathbf{B}_{us}$ is calculated as the average of the time-dependent magnetic field vector. The upstream ion velocity vector $\mathbf{V}_{us}$ and density N_{us} are taken as the sample values from the time series data whose time stamp falls within this 3.2 min period.

Because the ion velocity and density from VEX are available from AMDA at such low time resolution, these data are not suitable to be used for the Alfvén velocity. Therefore, another method to determine a Mach number for these shocks must be used. Following Zhang et al. (2008), the fast magnetosonic Mach number M_f is determined from the shock strength and θ_{Bn}, assuming the plasma is isotropic and Maxwellian both upstream and downstream. The Rankine-Hugoniot conditions (Kivelson & Russell, 1995) can be written as follows:

$$\frac{1}{2}+\frac{\beta\gamma}{2M_A^2(\gamma-1)}+\frac{\sin^2\theta_{Bn}}{M_A^2}=\frac{1}{2R_{cN}^2}+\frac{u^2}{2}+\frac{R_{cBz}\sin^2\theta_{Bn}}{M_A^2}+\frac{\gamma}{R_{cN}(\gamma-1)}\left[1-\frac{1}{R_{cN}}+\frac{\beta}{2M_A^2}-\frac{\left(R_{cBz}^2-1\right)\sin^2\theta_{Bn}}{2M_A^2}\right] \tag{11}$$

with

$$u = \frac{\sin\theta_{Bn}\cos\theta_{Bn}(R_{cN}-1)}{M_A^2 - R_{cN}\cos^2\theta_{Bn}} \tag{12}$$

the plasma density compression ratio R_{cN} is given by

$$R_{cN} = \frac{R_{cBz}M_A^2}{M_A^2 + \cos^2\theta_{Bn}(R_{cBz}-1)} \tag{13}$$

and R_{cBz} is the compression ratio of the magnetic field parallel to the shock front. It is assumed that $\beta = 1$ and the ratio of specific heats $\gamma = 5/3$. The equations are numerically solved for M_A from R_{cBz} and θ_{Bn}. The fast Mach number M_f is further calculated using $M_f = M_A(v_A/v_f)$, where

$$\frac{v_f^2}{v_A^2} = \frac{1}{2}\left[(1+\gamma\beta/2) + \sqrt{(1+\gamma\beta/2)^2 - 2\gamma\beta\cos^2\theta_{Bn}}\right] \tag{14}$$

The Rankine-Hugoniot relations imply that the normal components of the magnetic field in the asymptotically quiet upstream and downstream regions are equal. The normal component of the upstream magnetic field is obtained using the model shock normal. Accordingly, the downstream region is chosen as the 192-s period (within the analyzed 10-min downstream side) where the averaged value of $\mathbf{B}\cdot\mathbf{n}$ (i.e., normal component of B field) is closest to $\mathbf{B}_{us}\cdot\mathbf{n}$. From this interval, the downstream magnetic field vector $\mathbf{B}_{ds}$ is calculated as the average of the time-dependent magnetic field vector. Consequently R_{cBz} is found from:

$$R_{cBz} = \frac{|\mathbf{B}_{us} - (\mathbf{B}_{us}\cdot\mathbf{n})\,\mathbf{n}|}{|\mathbf{B}_{ds} - (\mathbf{B}_{ds}\cdot\mathbf{n})\,\mathbf{n}|} \tag{15}$$

The downstream ion velocity vector $\mathbf{V}_{ds}$ and density N_{ds} are taken as the sample values from the time series data whose time stamp falls within the same downstream 192-s period. Figure 8 gives an example of a plot of the Venusian bow shock as measured by VEX, and available in the SHARP database.

The SHARP database contains 1,660 Martian bow measurements by MAVEN between November 2014 and April 2017, and 2,776 Venusian bow shock measurements by VEX, measured between August 2008 and May 2009 (solar minimum) and between May 2011 and February 2012 (solar maximum). Table 1 lists the parameters available for MAVEN and VEX data.

4. Conclusions: Database Usage and Importance

The developed SHARP shock database contains crossings and parameters for 6,112 shocks, including 472 shocks observed at Cluster, 2,797 shocks at MMS, 407 at THEMIS/ARTEMIS, 1,660 at MAVEN, and 776 at VEX shocks. The basic shock parameters are calculated and available in the database for most of the shocks. The angle between the shock normal and the upstream magnetic field is estimated for all shocks. The Alfvénic Mach number is given for shocks observed at all spacecraft, except VEX. The SHARP shock database is able to facilitate numerous new studies of CSs both of a statistical nature as well as detailed case studies.

The database have already been utilized even at the stage of its development. The part of the database containing terrestrial shocks observed at Cluster was used to establish a proxy for the Alfvénic Mach number (Gedalin et al., 2021) right after it has been built. The proxy represented a simple dependence of the Alfvénic Mach number on a dimensionless parameter obtained from the magnetic field measurements only (from the mean upstream magnetic field B_u and the maximum magnetic field magnitude B_m).

The MMS section of the database has been used (Lalti et al., 2022) to determine the possible correlations between ion acceleration efficiency at shocks with different angles between the upstream magnetic field and the shock normal θ_{Bn} and the Alfvénic Mach number M_A. It was found that quasi-parallel shocks are more efficient at accelerating ions than quasi-perpendicular shocks but there is no definite correlation between the ion acceleration efficiency and M_A.

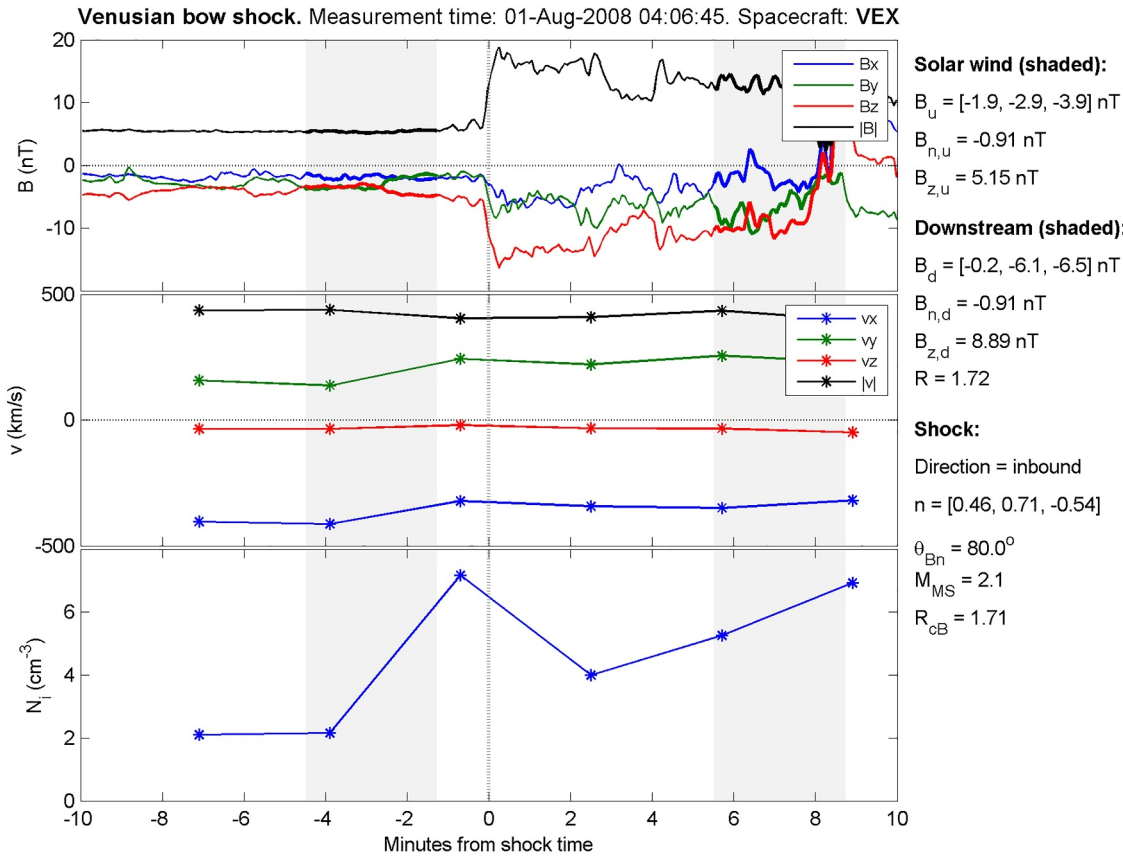

Figure 8. Example of a plot of the Venusian bow shock, measured by VEX. Upper panel: magnetic field strength. Middle panel: ion velocity. Lower panel: ion density.

Quite recently, the MMS part of the database was also used (Gedalin et al., 2023) in the analysis of the dependencies of the electron heating on the shock Mach number. It was found that the ratio between the downstream electron temperature and the incident ion energy decreases with the increase of the Mach number until it stabilizes at the level of several percent for $M_A \gtrsim 15$.

The latest development, based on the close inspection of the MMS section of the database and the corresponding shock plots, is the identification of shocks with persistent downstream fluctuations of the magnetic field in incorporation of this turbulence in the Rankine-Hugoniot relations (Gedalin, 2023a, 2023b).

By cataloging shocks based on various parameters, the database allows users to better understand the complicated dependence on shock parameters and their macro- and micro-scale structures. The database also provides plots which may be used by a researcher to visually choose shock(s) for further detailed analysis, according to the features in which the researcher is interested, for example, the magnetic profile, the ion or electron temperature evolution across the shock, or the waves in the vicinity of the shock transition.

The true merit/strength in the complete database is the ability to compare shocks in different parameter regimes. Figure 9 presents the ranges of Mach numbers and shock angles for the individual database sections (spacecraft) on the same axis to show what are the covered total parameter ranges and also where there are overlaps between the sections. The upper panel shows that the shock angle range is well covered by all spacecraft. The distributions are similar for Cluster, VEX, THEMIS, and MAVEN. For MMS the distribution is somewhat peculiar since the maximum is shifted toward oblique shocks near $\theta_{Bn} \sim 45°$. The difference between the MMS θ_{Bn} distribution and distributions for other spacecraft is caused by the difference in the procedures. MMS data analysis is the only using machine learning for crossing identification, and the only using OMNI data for the upstream parameters. This was done because of the large number of MMS shock crossings, almost 3,000. In other cases upstream and downstream regions are identified either visually or at certain time intervals around the shock. Same for Mach numbers. The same procedure as for Cluster was applied to MMS shocks when electron heating was studied

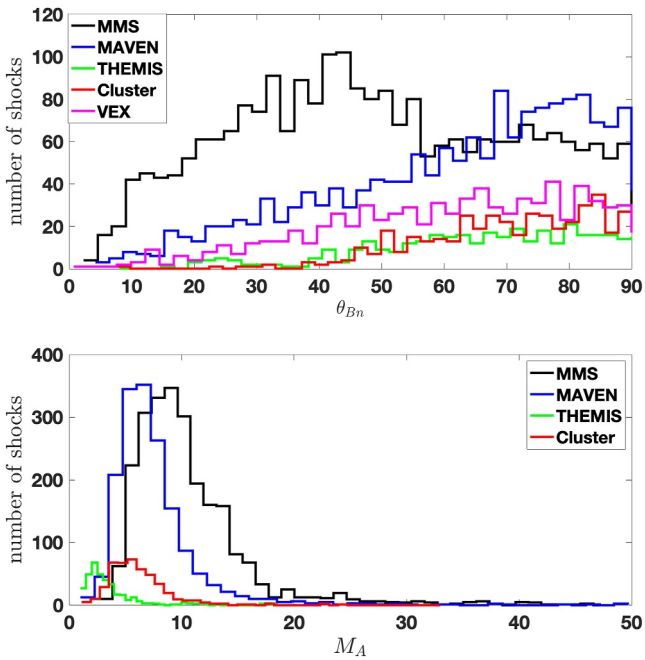

Figure 9. Upper panel: distribution of the shock angles θ_{Bn} as measured by five spacecraft and presented in five sections of the database. Bottom panel: distributions of the Alfvénic Mach numbers M_A in the four sections of the database (not available for VEX).

(Gedalin et al., 2023). This reduced the number of treatable shocks to about 500. Yet, there are many more crossings which may be useful for other studies. The adopted procedure allows a researcher to make selections on the base of approximately calculated parameters, even if some of them are not quite correct. Necessary corrections may and should be done during a specific study.

The bottom panel shows that the low-Mach number interplanetary shocks, covered by THEMIS section, nicely complement higher Mach number shocks by Cluster, MAVEN, and MMS. The overlap for these spacecraft promises great potential in studies of shocks with similar Mach numbers in different conditions or measured with different time resolution.

Figure 9 shows that there are fundamental differences in the parameter ranges for the different databases, even at the same terrestrial body. These differences arise from a number of factors. MAVEN measured lower solar wind speeds and substantially lower solar wind densities than MMS. Cluster and VEX observations were during solar cycle 23, while MAVEN was at Mars during cycle 24. The maximum in cycle 23 was substantially larger than in cycle 24. MMS shocks are also during cycle 24. Highest-Mach number MMS and MAVEN shocks correspond to very low magnetic fields but MAVEN densities are often by almost an order of magnitude lower.

The extensive SHARP shock database is a data product that contributes to the universal understanding of CSs since it provides a clear and efficient way of comparing terrestrial bow shock observations with shocks in other plasma environments (e.g., non-terrestrial planets, interplanetary shocks, astrophysical shocks). This can also facilitate collaboration between these sometimes distinct communities.

Data Availability Statement

The SHARP database is freely available at https://sharp.fmi.fi/shock-database/. The CLUSTER spacecraft data were obtained from the Cluster Science Archive, https://www.cosmos.esa.int/web/csa/. The list of shock crossing observed by Cluster CS1 was taken from https://www.cosmos.esa.int/web/csa/bow-shock-magnetopause-crossings. The MMS Science Data Center resides at https://lasp.colorado.edu/mms/sdc/public/. The THEMIS/ARTEMIS spacecraft data are obtained from: https://themis.igpp.ucla.edu/overview_data.shtml. The list of MAVEN shock measurement times was obtained from https://zenodo.org/records/6240624#.Y3djzS8w32c. The MAVEN and VEX data are obtained from the AMDA Versatile web tool for Space Physics, http://amda.cdpp.eu.

Acknowledgments

The SHARP project has received funding from the European Union's Horizon 2020 research and innovation programme under Grant agreement No 101004131. We thank Prof. Quanming Lu from University of Science and Technology of China, and Dr. Lican Shan from Institute Of Geology And Geophysics, China, for their valuable help with the list of VEX shocks.

References

Angelopoulos, V. (2008). The THEMIS mission. *Space Science Reviews*, *141*(1–4), 5–34. https://doi.org/10.1007/s11214-008-9336-1

Angelopoulos, V. (2011). The ARTEMIS mission. *Space Science Reviews*, *165*(1–4), 3–25. https://doi.org/10.1007/s11214-010-9687-2

Auster, H. U., Glassmeier, K. H., Magnes, W., Aydogar, O., Baumjohann, W., Constantinescu, D., et al. (2008). The THEMIS fluxgate magnetometer. *Space Science Reviews*, *141*(1–4), 235–264. https://doi.org/10.1007/s11214-008-9365-9

Balogh, A., Carr, C. M., Acuña, M. H., Dunlop, M. W., Beek, T. J., Brown, P., et al. (2001). The Cluster Magnetic Field investigation: Overview of in-flight performance and initial results. *Annales Geophysicae*, *19*(10/12), 1207–1217. https://doi.org/10.5194/angeo-19-1207-2001

Burch, J. L., Moore, T. E., Torbert, R. B., & Giles, B. L. (2016). Magnetospheric multiscale overview and science objectives. *Space Science Reviews*, *199*(1–4), 5–21. https://doi.org/10.1007/s11214-015-0164-9

Connerney, J. E. P., Espley, J., Lawton, P., Murphy, S., Odom, J., Oliversen, R., & Sheppard, D. (2015). The MAVEN magnetic field investigation. *Space Science Reviews*, *195*(1–4), 257–291. https://doi.org/10.1007/s11214-015-0169-4

Escoubet, C. P., Fehringer, M., & Goldstein, M. (2001). Introduction the cluster mission. *Annales Geophysicae*, *19*(10/12), 1197–1200. https://doi.org/10.5194/angeo-19-1197-2001

Farris, M. H., & Russell, C. T. (1994). Determining the standoff distance of the bow shock: Mach number dependence and use of models. *Journal of Geophysical Research*, *99*(A9), 17–17689. https://doi.org/10.1029/94JA01020

Garnier. (2022). Martian shock crossings dataset. *Zenodo*. https://doi.org/10.5281/zenodo.6240624

Gedalin, M. (2023a). Rankine–Hugoniot relations and magnetic field enhancement in turbulent shocks. *The Astrophysical Journal*, *958*(1), 2. https://doi.org/10.3847/1538-4357/ad0461

Gedalin, M. (2023b). Rankine-Hugoniot relations in turbulent shocks. *Frontiers in Physics*, *11*, 1325995. https://doi.org/10.3389/fphy.2023.1325995

Gedalin, M., Golan, M., Vink, J., Ganushkina, N., & Balikhin, M. (2023). Electron heating in shocks: Statistics and comparison. *Journal of Geophysical Research*, *128*(9), e2023JA031627. https://doi.org/10.1029/2023JA031627

Gedalin, M., Russell, C. T., & Dimmock, A. P. (2021). Shock Mach number estimates using incomplete measurements. *Journal of Geophysical Research: Space Physics*, *126*(10), e2021JA029519. https://doi.org/10.1029/2021JA029519

Gruesbeck, J. R., Espley, J. R., Connerney, J. E. P., DiBraccio, G. A., Soobiah, Y. I., Brain, D., et al. (2018). The three-dimensional bow shock of mars as observed by maven. *Journal of Geophysical Research: Space Physics*, *123*(6), 4542–4555. https://doi.org/10.1029/2018JA025366

Halekas, J. S., Taylor, E. R., Dalton, G., Johnson, G., Curtis, D. W., McFadden, J. P., et al. (2015). The solar wind ion analyzer for MAVEN. *Space Science Reviews*, *195*(1–4), 125–151. https://doi.org/10.1007/s11214-013-0029-z

Hall, B. E. S., Lester, M., Sánchez-Cano, B., Nichols, J. D., Andrews, D. J., Edberg, N. J. T., et al. (2016). Annual variations in the Martian bow shock location as observed by the Mars Express mission. *Journal of Geophysical Research: Space Physics*, *121*(11), 11474–11494. https://doi.org/10.1002/2016JA023316

Hall, B. E. S., Sánchez-Cano, B., Wild, J. A., Lester, M., & Holmström, M. (2019). The Martian bow shock over solar cycle 23–24 as observed by the Mars Express mission. *Journal of Geophysical Research: Space Physics*, *124*(6), 4761–4772. https://doi.org/10.1029/2018JA026404

Kivelson, M. G., & Russell, C. T. (1995). *Introduction to space physics*. Cambridge University Press.

Kruparova, O., Krupar, V., Šafránková, J., Němeček, Z., Maksimovic, M., Santolik, O., et al. (2019). Statistical survey of the terrestrial bow shock observed by the cluster spacecraft. *Journal of Geophysical Research: Space Physics*, *124*(3), 1539–1547. https://doi.org/10.1029/2018JA026272

Lalti, A., Khotyaintsev, Y. V., Dimmock, A. P., Johlander, A., Graham, D. B., & Olshevsky, V. (2022). A database of mms bow shock crossings compiled using machine learning. *Journal of Geophysical Research: Space Physics*, *127*(8), e2022JA030454. https://doi.org/10.1029/2022JA030454

McFadden, J. P., Carlson, C. W., Larson, D., Ludlam, M., Abiad, R., Elliott, B., et al. (2008). The THEMIS ESA Plasma Instrument and In-flight Calibration. *Space Science Reviews*, *141*(1–4), 277–302. https://doi.org/10.1007/s11214-008-9440-2

Olshevsky, V., Khotyaintsev, Y. V., Lalti, A., Divin, A., Delzanno, G. L., Anderzén, S. e. a., et al. (2021). Automated classification of plasma regions using 3D particle energy distributions. *Journal of Geophysical Research: Space Physics*, *126*(10), e2021JA029620. https://doi.org/10.1029/2021ja029620

Pollock, C., Moore, T., Jacques, A., Burch, J., Gliese, U., Saito, Y., et al. (2016). Fast plasma investigation for magnetospheric multiscale. *Space Science Reviews*, *199*(1–4), 331–406. https://doi.org/10.1007/s11214-016-0245-4

Rème, H., Aoustin, C., Bosqued, J. M., Dandouras, I., Lavraud, B., Sauvaud, J. A., et al. (2001). First multispacecraft ion measurements in and near the Earth's magnetosphere with the identical Cluster ion spectrometry (CIS) experiment. *Annales Geophysicae*, *19*(10/12), 1303–1354. https://doi.org/10.5194/angeo-19-1303-2001

Schwartz, S. J. (1998). Shock and discontinuity normals, Mach numbers, and related parameters. In G. Paschmann & P. Daly (Eds.), *Analysis methods for multi-spacecraft data*, *ISSI Scientific Reports Series* (Vol. 1, pp. 249–270).

Shan, L., Lu, Q., Mazelle, C., Huang, C., Zhang, T., Wu, M., et al. (2015). The shape of the Venusian bow shock at solar minimum and maximum: Revisit based on VEX observations. *Planetary and Space Science*, *109–110*, 32–37. https://doi.org/10.1016/j.pss.2015.01.004

Trotignon, J. G., Décréau, P. M. E., Rauch, J. L., Randriamboarison, O., Krasnoselskikh, V., Canu, P., et al. (2001). How to determine the thermal electron density and the magnetic field strength from the CLUSTER/WHISPER observations around the earth. *Annales Geophysicae*, *19*(10/12), 1711–1720. https://doi.org/10.5194/angeo-19-1711-2001

Zhang, T. L., Baumjohann, W., Delva, M., Auster, H.-U., Balogh, A., Russell, C., et al. (2006). Magnetic field investigation of the Venus plasma environment: Expected new results from Venus Express. *Planetary and Space Science*, *54*(13), 1336–1343. https://doi.org/10.1016/j.pss.2006.04.018

Zhang, T. L., Pope, S., Balikhin, M., Russell, C. T., Jian, L. K., Volwerk, M., et al. (2008). Venus Express observations of an atypically distant bow shock during the passage of an interplanetary coronal mass ejection. *Journal of Geophysical Research*, *113*(E9), E00B12. https://doi.org/10.1029/2008JE003128